

ANALYSIS OF THE BASIC DIAGRAM OF MAGNETIC-TRANSISTOR CONVERTERS

B. Abdullaev¹, Kh.E. Kholbutaeva², M.U. Idriskhodjaeva³, M.B. Peysenov⁴

¹Candidate of technical sciences, Associate Professor, Department of Electrical Engineering

²Senior teacher Department of Electrical Engineering

³Associate Professor, Department of Electrical Engineering

⁴Senior teacher Department of Electrical Engineering

^{1,2,3,4}Tashkent State Technical University

<https://doi.org/10.5281/zenodo.11093187>

Abstract. *The article provides an analysis of multiplying and dividing devices based on a magnetic transistor amplifier. We consider the amplification mode and the transient process of a magnetic transistor converter, and also provide a description of the operating states of the basic circuit. The proposed scheme is simple, economical, highly reliable, fast and stable. As a result of the research, based on the data obtained, characteristics were constructed on which it can be noted that the rate of change of induction during the operating half-cycle is constant and does not depend on the magnitude of the control signal. When designing functional converters with magnetic transistor pulse-width modulators, the one used in the analysis of one of the proposed circuits, taking into account the dynamic hysteresis loop, can serve as the basis for a preliminary assessment of the conversion accuracy in a given range of input values.*

Keywords: *converter, analysis, hysteresis loop, compensation, error, switching, generator, transient process, amplification mode, calculation, modulator, graphs, transistor, induction, magnetic permeability.*

A large class of multiplier-dividing devices and other functional converters are based on magnetic transistor amplifiers (MTAs), which act as pulse-width modulators. Converters with MTA are therefore called magnetic transistor (MP). In the existing literature [3,4,5], a general approach to the design of MP has not yet been developed, since the basic scheme of MP has not been defined and, as a consequence, there is no theoretical analysis of it. The choice of such a scheme and its selective study would make it possible to develop a unified methodology for calculating the MP, to identify the components of the error in the functional transformation and ways to compensate for them. Let's consider one of the possible variants of the basic MTA circuit (Fig. 1) on two cores A and B with power from a direct current source and transistor switching of the control windings w_y and working w_p from transformer T_p with circular frequency ω master oscillator (MO). The circuit is simple, economical, highly reliable, fast and stable, its operating states are determined by switching transistors T_1+T_4 are given in the table.

Table 1

Characteristics of the operating states of the circuit

Elements	State 1	State 2
Transistors T_1 and T_4	Open	Open
Transistors T_2 and T_3	Close	Close
Core A	Working half-cycle	Control half-cycle
Core B	Control half-cycle	Working half-cycle

Having accepted the known assumptions about the ideality of transistors and the rectangularity of the static hysteresis loop, we write the initial equations for the state 1:

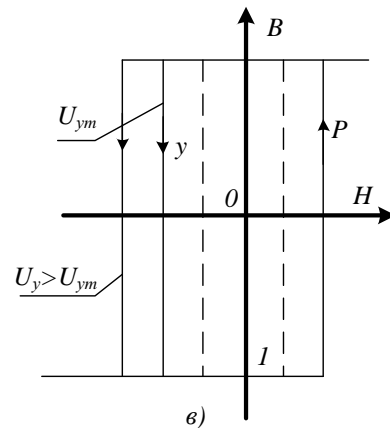
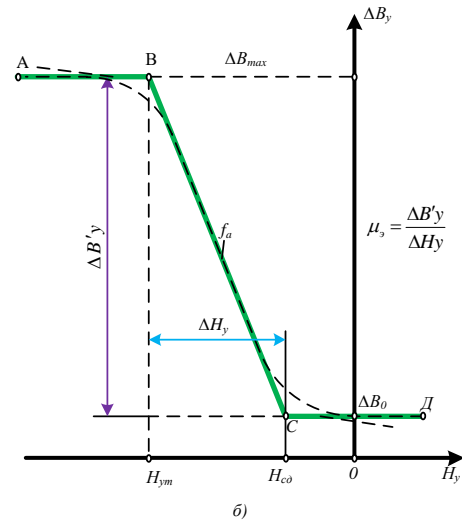
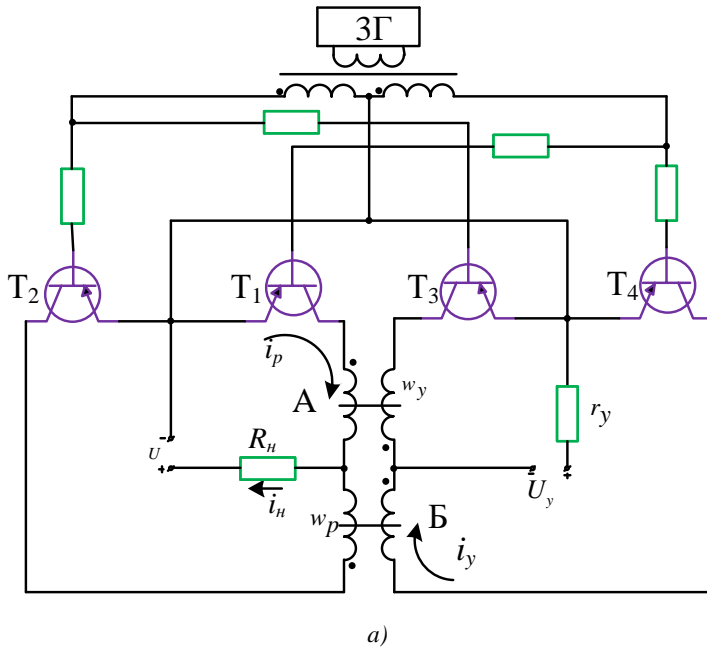
$$w_p S \omega \frac{dB_A}{d\tau} + i_p R_\Sigma = U_n, ; \quad (1)$$

$$w_y S \omega \frac{dB_B}{d\tau} + i_y R_y = U_y, \quad (2)$$

$$i_p w_p = H_A l; \quad (3)$$

$$-i_y w_y = H_B l; \quad (4)$$

where B_A, H_A и B_B, H_B – magnetic induction and field strength in cores A and B;



Rice. 1. Basic circuit of a magnetic transistor amplifier a); passage characteristic б); self-saturation area в).

U_n, i_p, R_Σ - supply voltage, current and total active resistance of the operating circuit; U_y, i_y, R_y - voltage, current and active resistance of the control circuit; S, l - core cross-section and length of the average magnetic field line.

Boost mode. The magnetization reversal of the cores occurs according to a particular dynamic cycle of the hysteresis loop, for which the expressions [2, 3] are valid:

$$\frac{dB}{d\tau} = \frac{\mu_3}{\pi} (H \mp H_C), \quad (5)$$

$$0 < |U_y| \leq |U_{yS}|, \quad (6)$$

where: μ_3 – equivalent magnetic permeability, determined from the dynamic demagnetization curve (DDR);

H_C – static coercive force;

Sign “-“ in formula (5) corresponds to an increase in induction in the core, “+” to its decrease. Then from equations (2) and (5) we obtain the expression for the control current:

$$i_y = \frac{U_y}{r_y} - \frac{x_3}{\pi r_y} \cdot \frac{L}{w_y k^2} (H_B + H_C). \quad (7)$$

Where $k = \frac{w_p}{w_y}$, $x_3 = \omega \frac{\mu_3 w_p^2 S}{L}$ - equivalent inductive reactance of the working winding.

Substituting expression (4) into (7), we obtain for the magnetic field strength of core B:

$$H_B = \frac{\frac{U_y w_y}{r_y l} - \frac{X_3 H_c}{\pi r_y w_y K^2}}{\frac{X_3}{\pi r_y K^2} - 1}. \quad (8)$$

Considering that the supply voltage of the MTA is

$$U = \frac{l}{w_p} (R_H + r_p) H_{pm}, \quad (9)$$

where H_{pm} - amplitude of the field strength in the operating half-cycle; from expressions (1), (5) and (9) we determine the strength of the core A:

$$H_A = \frac{H_{pm} (R_H + r_p) + x_3 \frac{H_c}{\pi}}{\frac{x_3}{\pi} + R_H + r_p}. \quad (10)$$

Then the expression for the operating circuit current is:

$$i_p = \frac{L}{w_p} \frac{H_{pm} \rho_x H_c}{1 + \rho_x}. \quad (11)$$

From expression (11) the current values in the operating circuit during magnetization intervals can be obtained ($0 + \alpha$) and saturation ($\alpha + \pi$). Really. When magnetized $x_3 \gg R_{\Sigma} \pi, \rho_x \rightarrow 0$, hence:

$$i_{p \text{ HOM}} \cong \frac{L}{w_p} H_c. \quad (12)$$

In the saturation interval $x_3 \rightarrow 0$, $\rho_x \rightarrow \infty$, in hence:

$$I_H = \lim_{\rho_x \rightarrow \infty} \frac{1}{w_p} \frac{H_{pm} \rho_x + H_c}{1 + \rho_x} = \frac{1}{w_p} H_{pm}. \quad (13)$$

From the point of view of the physics of processes, state 2 is not fundamentally different from state 1, cores A and B change roles, therefore we determine the average value of the load voltage over the period by integrating expressions (11) and (13):

$$U_{H.cp} = \frac{R_H l}{\pi w_p} \left[\frac{H_p m \rho_x + H_c}{1 + \rho_x} \alpha + H_p m (\pi - \alpha) \right]. \quad (14)$$

On the other hand, as for a conventional MU with self-saturation [1], for the MTA we can write:

$$U_{H.cp} = \eta U_{\text{вых cp}} - \eta (U - 2 f w_p s |\Delta B_y|), \quad (15)$$

where $\eta = \frac{R_H}{R_H + r_p}$; $|\Delta B_y|$ - the absolute value of the change in induction in the core during the control half-cycle.

Then, given that $U_n = 4fw_pSB_s$ From equations (14) and (15) we determine the MTA saturation angle:

$$\alpha = \frac{\pi(1+\rho_x)}{H_p m - H_c} \left\{ H_{pm} - \frac{2f\eta S w_p^2 [2B_s(1+\rho_x) - |\Delta B_y|]}{R_H l} \right\}. \quad (16)$$

To calculate the current and final values of the core inductions for state 1, we obtain

$$B_A = \frac{l(R_H + r_p)(H_{pm} - H_c)}{w_p^2 S \omega (1 + \rho_x)} (\tau - \theta_s) + B_s, \quad (17)$$

$$B_B = \frac{1}{w_y S \omega} \left[U_y + \frac{U_y - \frac{x_3 l H_c}{\pi w_y K^2}}{1 - \frac{x_3}{\pi r_y K^2}} \right] \tau + B_s, \quad (18)$$

where $0 \leq \tau \leq \alpha$; $U_y < 0$.

Passage characteristic of MTA. For DDR, we accept approximation by three straight segments (Fig. 1, b).

$$\begin{aligned} \Delta B_y &= \Delta B_0, \text{ on } (H_y \geq H_{c.d}); H_y < 0 \text{ (site C-D)}; \\ \Delta B_y &= \mu_0 (H_y + H_{cd}), \text{ on } (H_{ym} \leq H_y \leq H_{c.d}) \text{ (site B-C)}; \\ \Delta B_y &= \Delta B_{\max}, \text{ on } (H_y \leq H_{ym}) \text{ (участок A-B)}. \end{aligned}$$

Approximation parameters H_{ym} and H_{cd} can be determined directly from experimental DDR or theoretically. For example, H_{ym} is determined from formula (8) taking into account the fact that at the point «B» $U_{ym} = 4fS w_y B_s$;

$$H_{y.m.} = \frac{4fS w_y B_s - \frac{x_3 l H_c}{\pi r_y K^2}}{\frac{x_3}{\pi r_y K^2} - \frac{L}{w_y}}, \quad (19)$$

and the dynamic coercive force with a linear change in induction can be expressed as follows [3]

$$H_{cd} = H_c + 0,125\omega\delta d^2 B_s, \quad (20)$$

where δ - specific electrical conductivity of a ferromagnet;

d - thickness of the tape or plate.

To simplify, let's assume $B_{\max} = 2B_s$ и $B_{\max} \rightarrow 0$. Then for the SD section of the DDR, the voltage at the load is equal to $U_{\text{har}} = \tau U_n$, for site BC

$$U_{H.cp} = \tau (U_n - 2f w_p S |\mu_0|) (H_y - H_{Hcp}) \quad (21)$$

And for site AB

$$U_{Hcp} = R_H \frac{L}{w_p} H_{cd}. \quad (22)$$

The last expression indicates the horizontality of the left branch of the MTA pass characteristic, which is its feature compared to conventional self-saturation MU. This is explained

by the fact that when $|U_y| > 4fSw_yB_s$ the dynamic hysteresis loop becomes asymmetrical relative to the induction axis (fig.1,б), Moreover, no subsequent expansion of the loop is observed when the cores are magnetized, i.e. during the working half-cycle. Indeed, from equations (17) and (18) one can obtain the rate of change of induction for the working and control half-cycles:

$$\frac{dB_{rab}}{d\tau} = \frac{LR_s(H_{pm}-H_c)}{\omega^2Sw(1+\rho_x)}, \quad (23)$$

$$\frac{dB_{ynp}}{d\tau} = \frac{1}{w_yS\omega} \left(U_y - \frac{\frac{x_3 LH_c}{\pi w_y k^2}}{\frac{x_3}{\pi r_y k^2} - 1} \right). \quad (24)$$

Expression (23) shows that the rate of change of induction during the operating half-cycle is constant and does not depend on the magnitude of the control signal. Due to transistor switching of the windings at the end of the control half-cycle, the operating point of the MTA always returns to point I, from which the operating half-cycle begins, and at the maximum supply voltage, magnetization reversal occurs along a full hysteresis loop, which determines the constancy of the load current, equal to the no-load current of the MTA . This circumstance creates good prerequisites for the development of contactless magnetic relays with adjustable loop width while maintaining the differential coefficient unchanged.

To operate in amplification mode, as is known, a section of the VS DDR is used, in which the MTA has a voltage gain K_u , determined from expressions (8) and (21):

$$K_u = 2fw_p\mu_3\tau \frac{\pi w_y k^2}{L(x_3 - \pi r_y)}. \quad (25)$$

Transient processes in MTA. Keeping the previously accepted assumptions, we will assume that the control signal changes abruptly from the initial state U_y and satisfies condition (6). The most common case is when a control voltage jump occurs in the interval of a half-cycle of the master oscillator frequency, not coinciding with its end or beginning.

Let us assume that the moment of the jump τ_0 occurs within the (n-1) half-cycle, which is the control one for core A and the working one for B. At this point in time, the induction is equal B_A :

$$B_A/\tau_0 = \frac{1}{w_yS\omega} \left[U_{y0} - \frac{U_{y0} - \frac{x_3 LH_{cd}}{\pi w_y k^2}}{1 - \frac{x_3}{\pi r_y k^2}} \right] \tau_0 + B_s, \quad (26)$$

and the magnetic state of core A on the dynamic hysteresis loop is determined by point 1 (Fig. 2). Beginning with τ_0 , when

$$U_y = |U_{yT}| > |U_{y0}|,$$

the operating point moves along section 1-2, core A is demagnetized along a wider private cycle, and its induction changes as follows:

$$B_A/\tau_0 < \tau < (n-1)\pi = \frac{1}{w_yS\omega} \left[U_{y1} - \frac{U_{y0} - \frac{x_3 L}{\pi w_y k^2} H_{cd}}{\frac{x_3}{\pi r_y k^2} - 1} \right] \tau [(n-2)\pi + \tau_0] + \frac{B_A}{\tau_0}.$$

By the end of the half-period at $\tau = (n-1)\pi$ induction takes on the meaning:

$$B_A/(n-1)\pi = \frac{1}{w_yS\omega} \left[U_{yT} + \frac{\frac{x_3 LH_{cd}}{\pi w_y k^2}}{\frac{x_3}{\pi r_y k^2} - 1} \right] [(\pi - \tau_0)] + \frac{B_A}{\tau_0}. \quad (27)$$

Next in the half-cycle is working for core A and controlling for B. Core B is immediately remagnetized according to a new steady-state cycle corresponding U_y , at the end of the half-cycle its induction takes on a new steady-state value:

$$B_B/n\pi = \frac{1}{w_y S \omega} \left[U_{yT} + \frac{\frac{x_3 LH_{CD}}{\pi w_y k^2}}{\frac{x_3}{\pi r_y k^2} - 1} \right] \pi + B_S. \quad (28)$$

This is where the transient process for the voltage at the load ends.

In the next $(n+1)$ half-cycle, the representing point of the core A moves along the new steady cycle. The curves of the transition process in the MTA are shown in Figure 2. Thus, the duration of the transition process for average values is equal to:

$$\tau_{nn} = (\pi - \tau_0) + \pi = 2\pi - \tau_0, \quad (29)$$

the time of the transient process lies within one frequency period of the master oscillator.

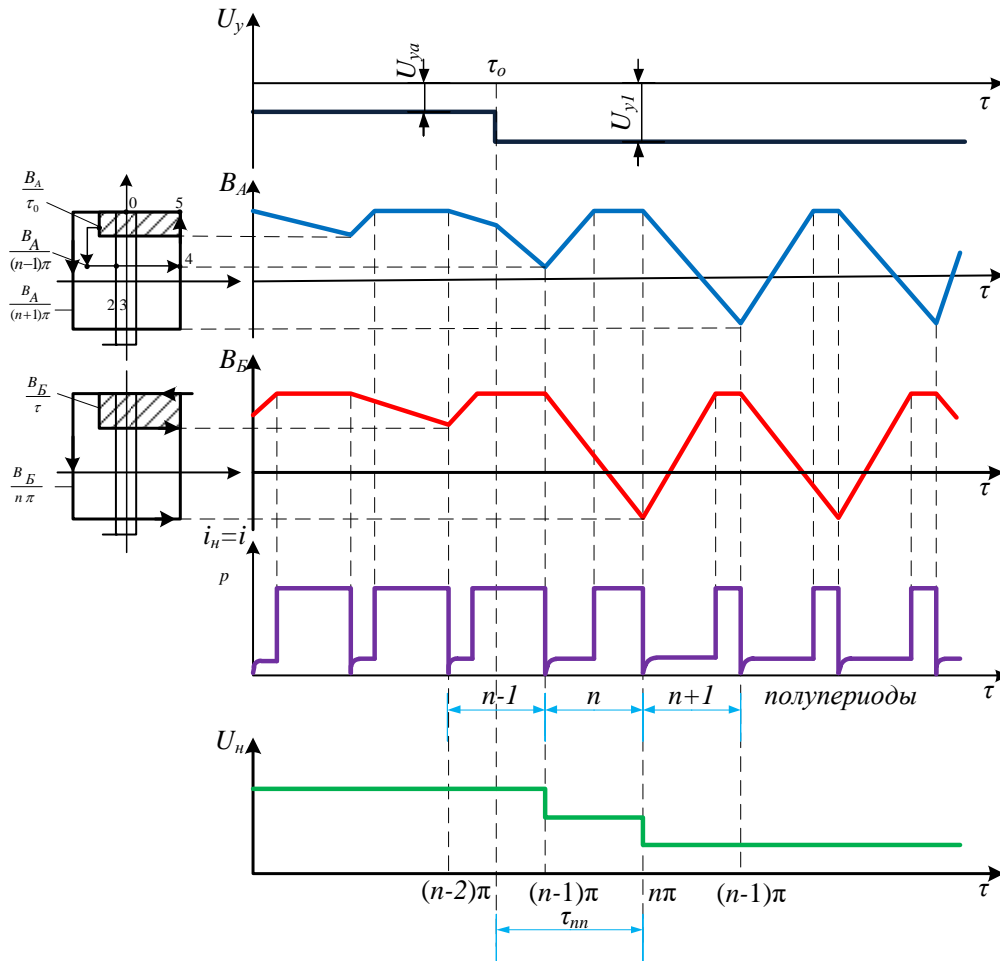


Fig. 2. Transition process

A particular case is when the control voltage jump coincides with the beginning of the $(n - 1)$ half-cycle. Then the representing point of the core A, already during this half-cycle, will move along a new established cycle, and the induction will change according to a linear law:

$$B_A = \frac{1}{w_y S \omega} \left[U_{y0} + \frac{U_{y0} \frac{x_3 LH_{CD}}{\pi w_y k^2}}{1 - \frac{x_3}{\pi r_y k^2}} \right] [\tau - (n - 2)\pi] + B_S. \quad (30)$$

Then, already in the next half-cycle, the voltage at the load will take its new steady-state value, and the MTA will be a link of pure delay by half the frequency period of the master oscillator.

The results of the analysis of one of the MTA circuits presented in the article, taking into account the dynamic hysteresis loop, can serve as the basis for the design of functional converters with magnetic transistor pulse-width modulators, in particular, for a preliminary assessment of the conversion accuracy in a given range of input values.

REFERENCES

1. Абдуллаев Б. Обобщенные модели пассивных нелинейных элементов электрических цепей и систем. Изд. ТашГТУ-2015. с.180.
2. Абдуллаев Б.А. Обобщенные модели и параметры пассивных нелинейных элементов электроэнергетических систем // Журнал Проблемы энерго- и ресурсосбережения - Т., 2013. № 3-4 – с. 161-167.
3. В.А. Abdullaev, А.А. Alimov, D.A. Xalmanov. To the problem of the calculation capacity of the nonlinear inductance // Seventh World Conference on Intelligent Systems.
4. Абдуллаев В., Холбутаева Х.Э., Идрисходжаева М.У. О методах коррекции качественных показателей преобразователей и элементов электрических цепей и систем. Электронный журнал «Инновации в нефтегазовой отрасли» №1/2020.-С.39-43.
5. Бегматов Ш.Э., Холбутаева Х.Э., Идрисходжаева М.У. Графо-аналитический способ построения статических характеристик вторичного источника электропитания. Евразийский союз ученых (ЕСУ) (ежемесячный научный журнал) №5(62). 2019. – С.36-39. DOI: 1031618ESU.2413-9335.2019.1.62.
6. N.Khamudkhanova, M.Idriskhodjaeva, Kh.Kholbutayeva. Construction principle of automatic control system adjustable multi-engine drive water lift pump unit. E3S Web of Conf., 384, 01057, (2023), <https://doi.org/10.1051/e3sconf/202338401057>
7. Abitkhodja Burkhankhodjaev, Malika Tuychieva, Elena Iksar, Kholjan Kholbutayeva, Baxtiyor Nurmatov. Investigation of the Energy Performance of electric Locomotives in Asymmetric Modes. AIP Conference Proceedings 2552, 030024 (2023), <https://doi.org/10.1063/5.0133920>
8. Abidov K.G., Zaripov O.O., Idriskhodjayeva M.U., Khamudkhanova N.B., and others. Specific Features of Operating Pumping Units and the Tasks of Ensuring Energy-Saving Modes of Operation by Controlling Them. AIP Conference Proceedings, 2552, 030022, 2022. <https://doi.org/10.1063/5.0112384>
9. Burkhanhodjaev, A., Iksar, E, Idriskhodjayeva M. An algorithm for controlling a traction asynchronous drive that minimizes electrical power losses. E3S Web of Conferences, 216, статья № 01107, <https://www.scopus.com/authid/detail.uri?authorId=57221167017&eid=2-s2.0-85098453474>
10. Shavkat Begmatov, Saidakhon Dushmanamedova, Kholzhon Holbutaeva. Study of ferro resonance using generalized models of passive nonlinear elements. E3S Web of Conferences 216, 01115 (2020). <https://doi.org/10.1051/e3sconf/202021601115>
11. R Karimov, M Bobojanov, N Tairova, X Xolbutayeva, A Egamov and N Shamsiyeva. Non-contact controlled voltage stabilizer for power supply of household consumers. IOP Conf. Series: Materials Science and Engineering 883 (2020) 012120. doi:10.1088/1757-899X/883/1/012120